DEVELOPMENT OF NEW RHEOLOGICAL TOOLS FOR ASPHALT BINDER AND CONCRETE CHARACTERIZATION

June 2006

Montgomery T. Shaw, Principal Investigator
Patrick T. Mather, Co-Principal Investigator
Antonio E. Senador, Graduate Research Assistant
Yatin Patil, Graduate Research Assistant

JHR 06-306 Project 03-7

This research was sponsored by the Joint Highway Research Advisory Council (JHRAC) of the University of Connecticut and the Connecticut Department of Transportation and was performed through the Connecticut Transportation Institute of the University of Connecticut.

Technical Report Documentation Page

1. Report No.	2. Government Accession No.	3. Recipient's Catalog No.
JHR 06-306	N/A	

4. Title and Subtitle	5. Report Date
Development of New Rheological Tools for Asphalt Binder and Concrete Characterization	June 2006
	6. Performing Organization Code: JH 03-7

7. Author(s)	8. Performing Organization Report No.
Montgomery T. Shaw	JHR 06-306

9. Performing Organization Name and Address	10. Work Unit No. (TRAIS)
University of Connecticut Connecticut Transportation Institute Storrs, CT 06269-5202	N/A
	11. Contract or Grant No.: N/A

12. Sponsoring Agency Name and Address	13. Type of Report and Period Covered
Connecticut Department of Transportation 280 West Street Rocky Hill, CT 06067-0207	
	14. Sponsoring Agency Code: JH 03-7

15. Supplementary Notes

This study was conducted under the Connecticut Cooperative Highway Research Program (CCHRP, http://www.engr.uconn.edu/ti/Research/crp_home.html).

16. Abstract

The goal of this project was to develop and test new methods for measuring the flow properties of asphalt and asphalt concretes in an expeditious manner. The work was concentrated on the design and construction of a novel combinatorial rheometer that was exploited the squeeze-flow geometry. With a two-dimensional combinatorial array, variable such as temperature and asphalt type could be covered rapidly. A prototype featuring nine stations and a 30 °C temperature gradient was fabricated and tested over a wide range of stresses. The results agreed substantially with properties measured using conventional rheometry.

17. Key Words	18. Distribution Statement
Squeeze flow, combinatorial rheometer, asphalt rheology	No restrictions. This document is available to the public through the National Technical Information Service Springfield, Virginia 22161

19. Security Classif. (of this report)	20. Security Classif. (of this page)	21. No. of Pages	22. Price
Unclassified	Unclassified	25	N/A

Form DOT F 1700.7 (8-72) Reproduction of completed page authorized

Acknowledgements

The authors would like to acknowledge the able technical assistance of Robert Bouchard and Matthew Beebe for help with the design and fabrication of the combinatorial rheometer. Dr. James Mahoney in the Connecticut Advanced Pavement (CAP) Laboratory supplied characterized asphalt samples, for which we are most grateful. We are indebted to the staff of the Connecticut Transportation Institute, especially Stephanie Merrall, for reminders about due dates and other procedural matters.

SI* (MODERN METRIC) CONVERSION FACTORS

APPROXIMATE CONVERSIONS TO SI UNITS

SYMBOL	WHEN YOU KNOW	MULTIPLY BY	TO FIND	SYMBOL
		LENGTH		
in	inches	25.4	millimeters	mm
ft	feet	0.305	meters	m
yd	yards	0.914	meters	m
mi	miles	1.61	kilometers	km
		AREA		
in^2	square inches	645.2	square millimeters	mm^2
ft^2	square feet	0.093	square meters	m^2
yd^2	square yard	0.836	square meters	m^2
ac	acres	0.405	hectares	ha
mi^2	square miles	2.59	square kilometers	km^2
		VOLUME		
fl oz	fluid ounces	29.57	milliliters	mL
gal	gallons	3.785	liters	L
ft^3	cubic feet	0.028	cubic meters	m^3
yd^3	cubic yards	0.765	cubic meters	m^3
		NOTE: volumes greater than 1000 L shall be shown in m^3		
		MASS		
oz	ounces	28.35	grams	g
lb	pounds	0.454	kilograms	kg
T	short tons (2000 lb)	0.907	megagrams (or "metric ton")	Mg (or "t")
		TEMPERATURE (exact degrees)		
°F	Fahrenheit	5 (F-32)/9 or (F-32)/1.8	Celsius	°C
		ILLUMINATION		
fc	foot-candles	10.76	lux	lx
fl	foot-Lamberts	3.426	$candela/m^2$	cd/m^2
		FORCE and PRESSURE or STRESS		
lbf	poundforce	4.45	newtons	N
lbf/in^2	poundforce per square inch	6.89	kilopascals	kPa

APPROXIMATE CONVERSIONS FROM SI UNITS

SYMBOL	WHEN YOU KNOW	MULTIPLY BY	TO FIND	SYMBOL
		LENGTH		
mm	millimeters	0.039	inches	in
m	meters	3.28	feet	ft
m	meters	1.09	yards	yd
km	kilometers	0.621	miles	mi
		AREA		
mm^2	square millimeters	0.0016	square inches	in^2
m^2	square meters	10.764	square feet	ft^2
m^2	square meters	1.195	square yards	yd^2
ha	hectares	2.47	acres	ac
km^2	square kilometers	0.386	square miles	mi^2
		VOLUME		
mL	milliliters	0.034	fluid ounces	fl oz
L	liters	0.264	gallons	gal
m^3	cubic meters	35.314	cubic feet	ft^3
m^3	cubic meters	1.307	cubic yards	yd^3
		MASS		
g	grams	0.035	ounces	oz
kg	kilograms	2.202	pounds	lb
Mg (or "t")	megagrams (or "metric ton")	1.103	short tons (2000 lb)	T
		TEMPERATURE (exact degrees)		
°C	Celsius	1.8C+32	Fahrenheit	°F
		ILLUMINATION		
lx	lux	0.0929	foot-candles	fc
cd/m^2	$candela/m^2$	0.2919	foot-Lamberts	fl
		FORCE and PRESSURE or STRESS		
N	newtons	0.225	poundforce	lbf
kPa	kilopascals	0.145	poundforce per square inch	lbf/in^2

*SI is the symbol for the International System of Units. Appropriate rounding should be made to comply with Section 4 of ASTM E380.
(Revised March 2003)

Table of Contents

List of Figures

List of Tables

List of Photographs

(See Figures that are part of Figures 3 and 4)

Definitions of Terms

Term or acronym	Definition
Aliphatic	Stable organic chemical structure similar to paraffin wax
Aromatic	Organic structure featuring carbon in the form of rings. Benzene is an aromatic compound
Dynamic flow	Refers here to oscillatory torsional deformation of a disk-shaped sample between two parallel disks.
Fluorocarbon	Refers to a organic structure in which some or all of the hydrogen atoms are replaced by fluorine. Teflon is an example
Lubrication limit	State where the only hydrodynamic terms of importance is due to viscous forces resulting from velocity gradients across a small gap
Newtonian	An adjective used to describe a viscous fluid with a constant viscosity
Polyethylene terephthalate	A polyester sold under such trade names as Mylar®
PET	Polyethylene terephthalate
Power-law fluid	Shear-thinning viscous fluid defined by Equation 7
SLR	Single-lens reflex (camera)
TMA	Thermomechanical analyzer. An instrument designed to measure length changes in solid samples as the temperature is changed.
Wavy washer	Thin spring washer bent into a wave form with three peaks

Symbols

Symbol	Definition
a	$(3n + 5)/2n$
F	Applied force in squeezing-flow experiment
H	Total gap in squeezing flow, also the thickness of the sample
H_0	Initial gap in squeeze-flow experiment
$\dot{H}$	Same as $-dH/dt$
K	Constant defined by Equation 6
n	Parameter in power-law fluid model
m	Parameter in power-law fluid model
R	Radius of sample in squeezing flow
T	Temperature
T_0	Reference temperature in Equation 1
V	Volume of sample in Type B squeeze-flow experiment
$-dH/dt$	Closing velocity in squeezing flow
α	Thermal expansion coefficient
ρ	Density
$\dot{\gamma}$	Magnitude of shear rate
η	Shear viscosity
$\lvert\eta^*\rvert$	Magnitude of complex viscosity in dynamic experiment defined as magnitude of dynamic shear stress divided by the magnitude of the dynamic shear rate
ω	Frequency (rad/s) in dynamic oscillatory flow

Development of New Rheological Tools for Asphalt Binder and Concrete Characterization

Introduction

Asphalt, the heavy feedstock from petrochemical refineries, is predominantly used as a binder for roads. Its properties depend on the composition of the feed stock and the processing parameters. Not surprisingly, it is a complex material containing aliphatic and aromatic, saturated and unsaturated, polar and non-polar organic compounds. The supermolecular structure is thought to be a three-dimensional network of asphaltenes dispersed in maltenes.[1] Asphaltenes comprise the hexane- or heptane-insoluble fraction, and are aggregates of polar aromatic compounds.[2] Maltenes, on the other hand, are non-polar aliphatic hydrocarbons soluble in hexane or heptane.

Asphalt is graded for a particular temperature range as a road binder using standardized mechanical tests.[3] These tests, though simple in concept, involve expensive equipment and are exceedingly time consuming. The tests are protracted mainly because asphalt undergoes considerable structural changes due to physical aging.[4,5] Work done by other groups has shown that asphalt requires isothermal annealing for extended periods (>10 h) prior to rheological measurements,[6] thus consuming valuable instrument time. Because of their codification, the conventional tests will be continue to be used. However, considerable time could be saved by a quick prescreeing process to eliminate batches of asphalt that are unlikely to meet the required specifications. A simpler, quicker test is needed.

No matter how simple the test, conventional rheometers lack the ability to characterize multiple samples simultaneously and most require that the sample be annealed in the fixtures. To alleviate this problem there is a need for simultaneous analysis of materials under an array of test variables. With such a procedure, one can test samples in a combinatorial fashion under a stress and temperature gradient in minutes per sample, as opposed to hours required by conventional rheometers. Multiple samples can be analyzed and compared in a single experimental run, which can reduce error connected with resolving small differences between the samples. The combinatorial approach is broadly applied in synthesis, but for characterization it is not so popular. Only one study has been reported for parallel rheological characterization of polymer solutions.[7] So far no experimental study has been reported on combinatorial rheological characterization of solids or melts.

One of the off-Broadway methods used for characterizing materials is squeeze flow.[8-26] While its nonuniform, transient flow field has discouraged commercialization, it does have several distinct advantages for testing asphalt. For example, the sample is placed between two disposable plates meaning that all sample preparation, loading and annealing can be done externally to the rheometer. In a real sense, this makes the test, relative to conventional rheometry, analagous to the cartridge rifle as opposed to a muzzle loader.

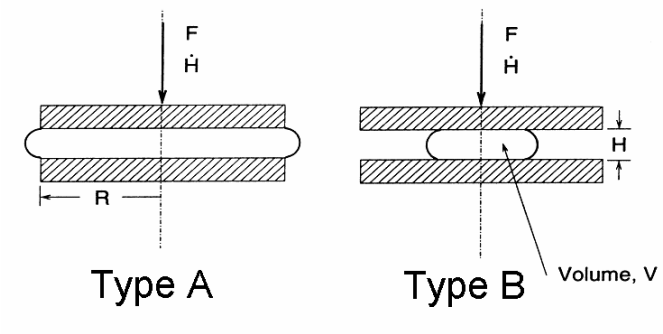

Figure 1. Squeeze-flow geometries. Type A features a fixed radius, whereas Type B uses a fixed sample volume. Type B was used for this study

Most squeeze flow geometries involve radial flow of disc-shaped samples between two parallel plates under a constant normal force or constant approach velocity. By measuring the applied load, sample volume and the change in the thickness as a function of time, shear stress and shear rate can be approximated. Two types of squeeze flow, namely constant diameter (Type A) and constant volume (Type B), have been reported; these are illustrated in Figure 1. In the Type A geometry the diameters of the sample and plates are same; the material squeezed out of the plates is ignored. The majority of the squeeze flow studies reported are based on Type A squeeze flow. In constant-volume squeeze flow the sample diameter is smaller than the plate diameter and material never flows out of the plates; thus the volume of sample subjected to force remains same. An advantage of this geometry is that one can track either the decrease in gap or increase in sample radius, whereas the constant-diameter method requires direct measurement of the gap. For the squeezing of a power-law fluid in this geometry, and analytical solution known as the Scott equation applies in the lubrication-approximation limit.[9] The lubrication limit is achieved when the gap is small compared to the radius. With the Type B geometry, there are some issues with respect to the treatment of the volume occupied by the bulge at the flow front, but these are less important with thin gaps.

The objective of this work was to develop a fast and a simple combinatorial setup for parallel characterization of asphalt under an array of test variables. Using constant-volume squeeze flow, multiple samples in a temperature gradient arrangement were simultaneously subjected to squeeze flow to assess their rheological behavior. The results obtained using combinatorial setup were then compared with those obtained using torsional dynamic flow between parallel plates in an ARES rheometer. The ARES rheometer, currently manufactured by TA Instruments, is a high-end research instrument that operates in the controlled-strain mode over an extremely broad range of temperature and frequency.

Experimental:

Instrumental Setup:

Figures 2A & 2B shows the combinatorial setup used for this study. The vacuum port in plate ‘a’ connects to a vacuum pump. A large flask was placed in the vacuum line to

allow rapid application of vacuum. A mercury manometer was used to check the applied vacuum, while a vacuum regular provided control over the pressure and thus the force on the membrane. A thin transparent polyethylene terephthalate film was placed between plates 'b' and 'c' to hold vacuum. Rubber gaskets were placed between plates 'a' and 'b' and plates 'b' and 'c' to prevent leakage. Eight Allen screws fastened the three plates together. For all experiments the applied vacuum was 76 mm Hg, for a pressure differential across the membrane of 90 kPa. A temperature gradient was achieved by circulating hot and cold water through four channels drilled in plate 'a'. Nine circular cavities, 1 mm deep, were machined in plate 'a' to position the samples. Thermocouples were embedded in plate 'a' below each sample cavity. Before the experiment, dummy asphalt samples, each containing thin thermocouples, were sandwiched between two circular cover slips and placed in the sample cavities. After applying vacuum and achieving the desired plate temperature gradient, both the sample temperatures and plate temperatures below each sample cavity were measured. This procedure provided a correction for the sample temperature relative to the plate temperature. The entire setup was placed in insulating foam. Sample diameters were recorded at desired intervals using a Nikon D70 digital SLR camera. The camera was connected to a computer via a USB and was controlled by Nikon Capture 4 camera control software. Every image file had embedded time information, which was used for shear-rate calculation.

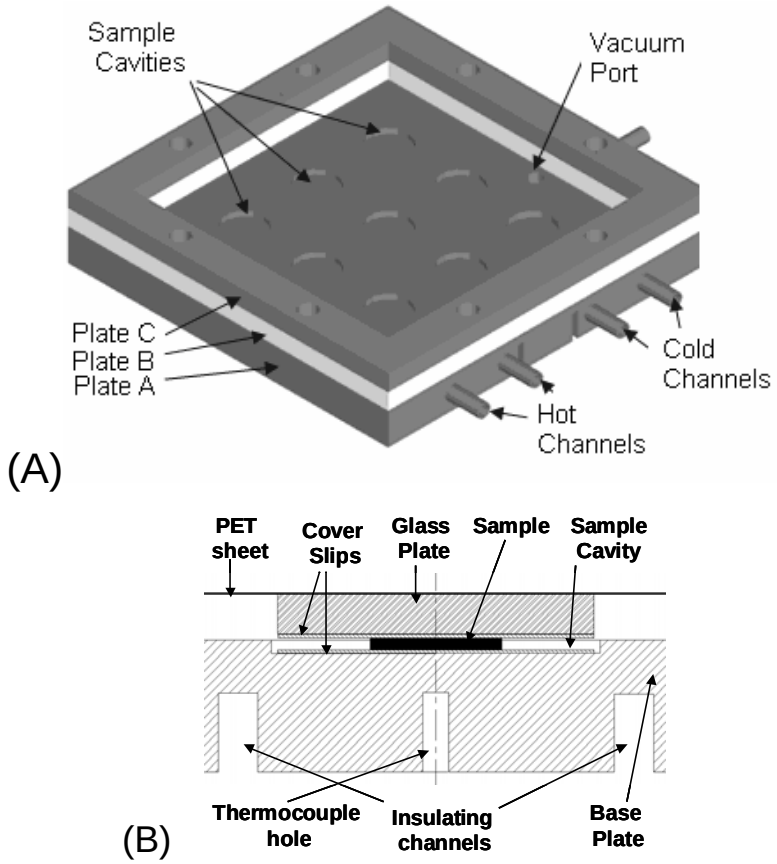

Figure 2. Combinatorial instrumental setup. Array (A), and cross section of unit cell (B)

Sample preparation:

Standardized asphalt samples were obtained from Connecticut Advanced Pavement Laboratory.[27] As asphalt is very difficult to handle, we adopted a form-and-freeze technique to prepare the required disk-shaped test units. In 0.5-, 1- and 1.5-mm-thick aluminum plates, 6-, 9-, 12- and 15-mm holes were drilled to serve as molds to make the asphalt disks. The plates were coated with a mold-release agent Chemlease-PMR from Chem-Trend Release Innovations. The plate, along with the asphalt, was placed between two Teflon sheets and kept in a hot press for 10 min at 60 ^{o}C. After removing the assembly from hot press it was cooled in dry ice for 5 min. The asphalt disks were ejected under cold conditions, and placed between two pre-weighed cover slips. These sandwiches were annealed at 60 ^{o}C for 5 min. After cooling the specimens were weighed and placed in the combinatorial setup. The sample volume was calculated from its weight and density.

Test procedure:

The temperatures of the water baths were adjusted to achieve the desired temperature gradients. The discs were placed in the sample cavities for 20 min to equilibrate with the plate temperature. After clamping the three plates, the image acquisition was started, followed by application of vacuum. The experiment was continued for 20 min. The pixel area of each sample was measured by using Image J 1.34S image analysis software available from the National Institutes of Health website. A metal disc of known diameter was placed in the setup as a calibration standard. The sample thickness was computed from the sample area, weight and density. The sample diameters and thicknesses in an array were selected to cover a wide shear rate range.

Density at elevated temperature:

Asphalt density in the range of 30 to 70 ^{o}C was measured using a dilatometer accessory in a Perkin Elmer Thermo Mechanical Analyzer TMA-7. The dilatometer dimensions were measured and it was filled with asphalt sample PG 76-28. The sample was heated, cooled and reheated from 30 to 70 ^{o}C at rate of 1 ^{o}C/min. The density values obtained from the second heating run shown in Figure 3 were used for thickness calculations. Assuming a constant expansion coefficient gives the result

$$\rho = \rho_0 \exp[-\alpha(T - T_0)] \tag{1}$$

with α = 0.00107 K^{-1}, and ρ_0 = 1.0344 g/cm^3 at a T_0 of 30 °C.

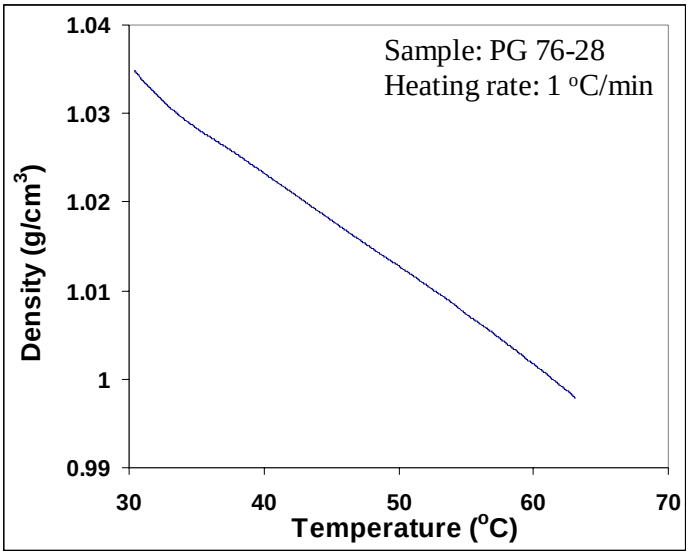

Figure 3. Asphalt density. Shown is the density of PG 76-28 asphalt over the test temperature range.

Force computation:

The force experienced by each sample under an applied vacuum was estimated based on the deflection of calibrated wavy washers. A load vs. deflection calibration curve was recorded beforehand for each washer using an Instron tensile tester. Sequentially at each sample site, a calibrated washer and a pre-weighed aliquot of silicone polymer (SE 30) were placed between two glass cover slips. A 25-mm-diameter, 4-mm-thick glass plate was placed on top of the cover slips. By starting with a zero-force reading, the deflection of the wavy washer should equal the decrease in the thickness of the polymer after application of vacuum and waiting long enough for the polymer to relax completely. The decrease in the thickness was computed by measuring the increase in the area of the polymer, assuming that the sample volume does not change. As with the asphalt samples, the area before and after application of vacuum was measured by taking pictures using a digital camera (Figure4a). During these experiments the other sample cavities had cover slips and glass plates to position the membrane correctly. Figure 4b shows the average value of the force experienced by the nine samples and their positions in the setup. The force experienced by the center sample is highest as the PET film has minimum edge constraints at this position. Clearly in a larger array, the forces at each station would be virtually constant.

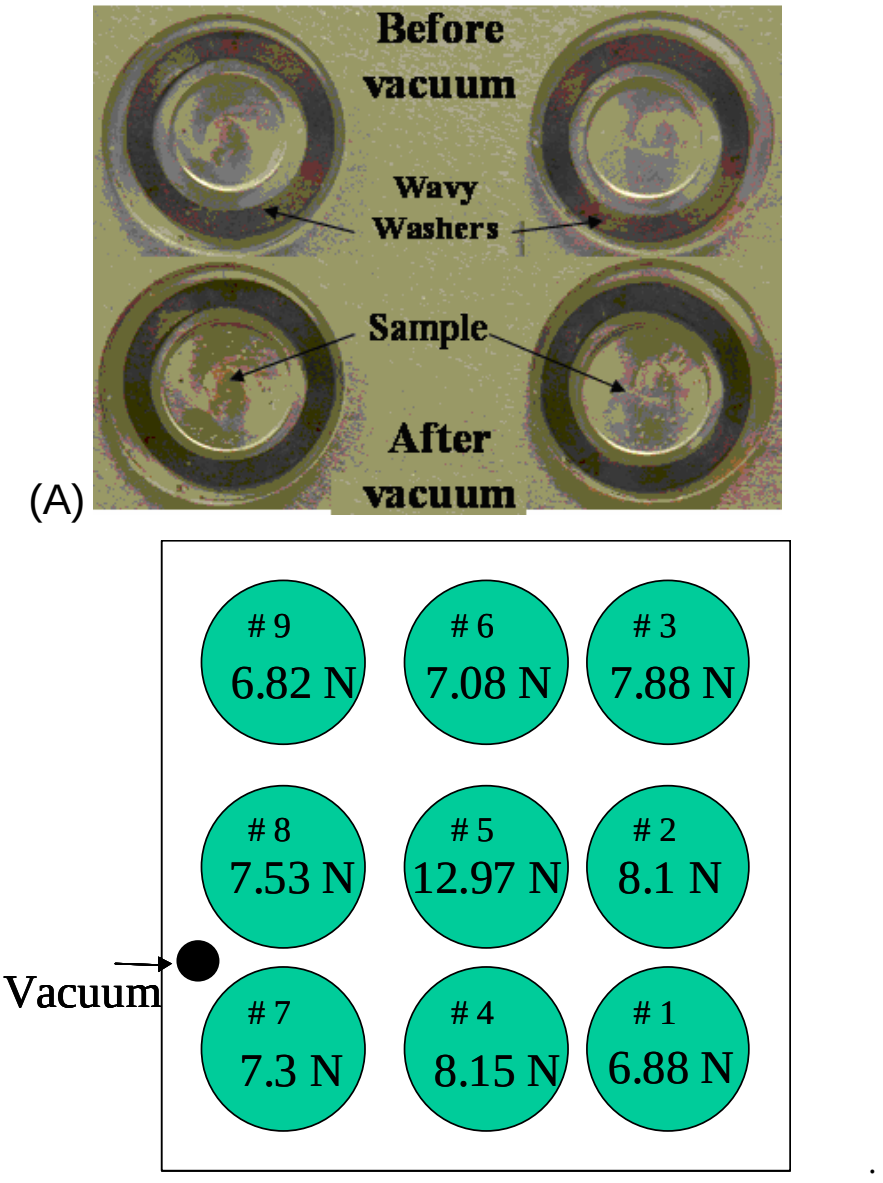

Figure 4. Force calibration. (A) Photo of silicone samples in the center of wavy washers being squeezed in the combinatorial rheometer for force calibration; and (B) resulting forces with a pressure difference of 90 kPa across the membrane.

Result and discussions:

Figure 5 shows the images recorded during a squeeze-flow run. The samples on the right side of the images had hot water channels below them and those on the left side had cold-water channels. The sample temperatures for the three arrays measured by placing dummy asphalt samples were 20, 40 and 61 ^{o}C. After application of vacuum, some of the samples over a period of time squeezed out of the disc and the data beyond that point was not considered in the analysis. The samples along the low-temperature side did not reach

the edge of the disc. The increase in the sample area obtained from image analysis is shown in Figure 6. The data sets that appear truncated are those where the sample reached the edge of the discs, and the logging of data was discontinued.

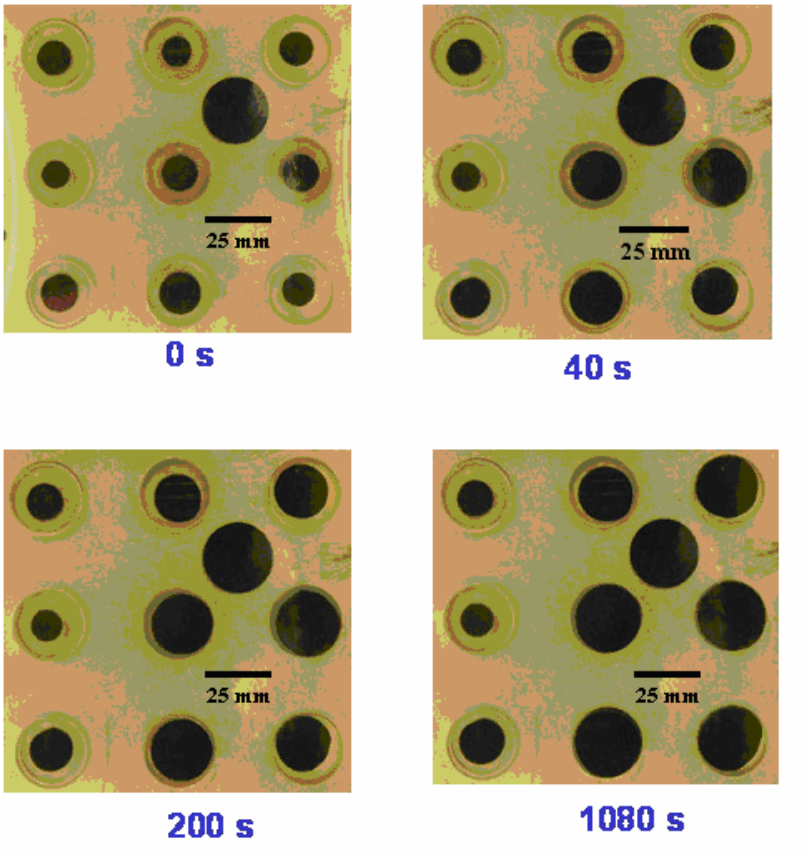

Figure 5. Squeeze flow run. Images taken at the times indicated. Applied pressure difference was 90 kPa; temperatures of the array columns were 20, 40 and 61 ^{o}C from left to right.

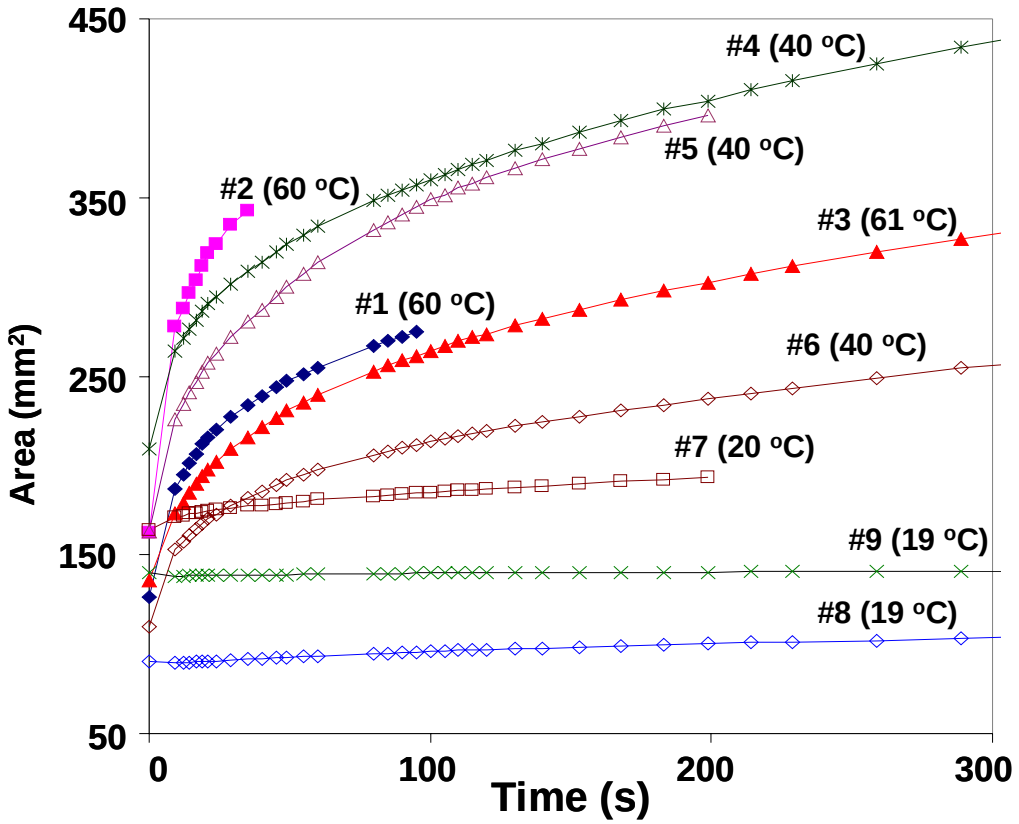

Figure 6. Sample area data during a run. These were calculated from recorded images of array during a single combinatorial squeeze flow experiment.

The sets of data thus obtained were used to compute the thickness of the samples as a function of time. Using area, density and weight of individual samples, the thickness calculated as a function of time is shown in Figure 7. As expected, the initial thicknesses of the cold samples were close to the thickness of the mold used to form them. However samples at elevated temperatures exhibited lower thickness than their mold thickness, as they experience some flow during the setup due to low viscosities.

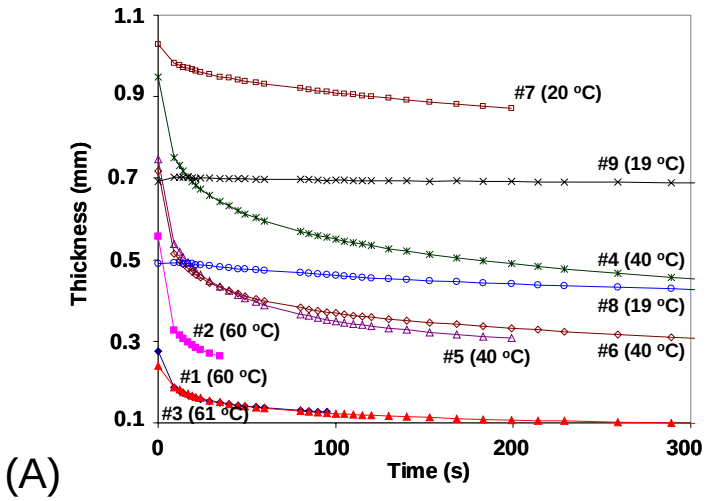

(A)

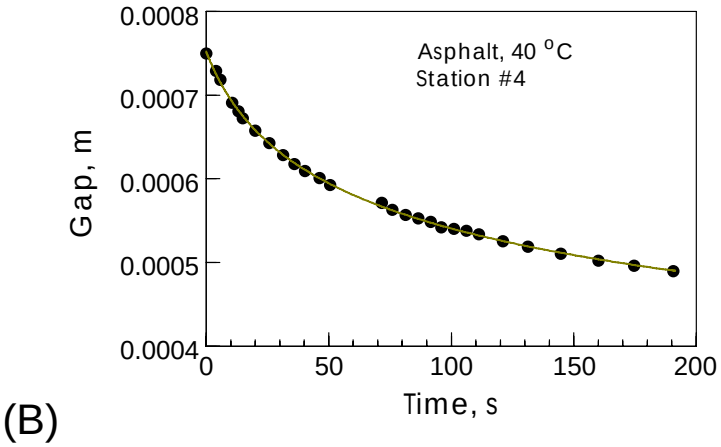

(B)

Figure 7. Change of gap with time. (a) Sample thicknesses derived from area data of Figure 6; and (b) example fit of Scott equation (Eq. 4) to results for Site #4. The first point has been eliminated and the time scale shifted. Power-law constants: m = 7070 ± 400 and n = 0.572 ± 0.024. Initial gap H_0 = 0.735 ± 0.008 mm.

Based on constant-volume squeeze flow equations, the rim shear rate and rim shear stress were calculated as follows.[28]

$$\sigma_R = \left[\frac{n+3}{4}\right]\left[\frac{H^{5/2}F}{\pi\left(V/\pi\right)^{3/2}}\right] \tag{2}$$

$$\dot{\gamma}_R = \left[\frac{2\left(2n+1\right)}{3n\,2^{1/n}}\right]\left[\frac{3\left(-dH/dt\right)\left(V/\pi\right)^{1/2}}{2H^{5/2}}\right] \tag{3}$$

Here n is the power-law exponent (equation 6), H is the sample thickness at time t, F is the applied force and V is the volume of the sample. The value of n may be calculated from the slope of a plot of log ($-dH/dt$) vs. log H and allowed to change with time as the gap closes. For a power-law fluid, such a plot yields a straight line (Scott equation) with a slope of $5(n+1)/2n$, from which the power law index is calculated. The disadvantage of this approach is that the gap data must be differentiated twice—once to get dH/dt and again to get the final value of n—which is likely to increase error. Alternatively, one can assume that the power-law parameters are invariant with time and integrate the Scott equation

$$F = \frac{(-\dot{H})^n}{H^{\frac{5(n+1)}{2}}}\left(\frac{2n+1}{2n}\right)^n \frac{2^{n+1}\pi}{n+3}\left(\frac{V}{\pi}\right)^{\frac{n+3}{2}} m \tag{4}$$

to yield:

$$H(t;m,n) = \frac{H_0}{\left[1 + H_0^a Kat\right]^{1/a}} \tag{5}$$

where H_0 is the initial gap, a =(3n +5)/2n, and K is given by the equation

$$K = \frac{2n}{2n+1}\left[\frac{(n+3)F}{\pi m(V/\pi)^{\frac{n+3}{2}} 2^{n+1}}\right]^{1/n} \tag{6}$$

The symbol m is the proportionality constant in the usual power-law expression

$$\eta = m\dot{\gamma}^{n-1} \tag{7}$$

where η is the viscosity and $\dot{\gamma}$ is the magnitude of the shear rate. One can then find m and n by nonlinear regression of the gap vs. time data using Equations 5 and 6. The initial gap H_0 can also be treated as a parameter, as it may not be known very accurately. Note that any time can be used as zero time and the corresponding gap at that time will be H_0.

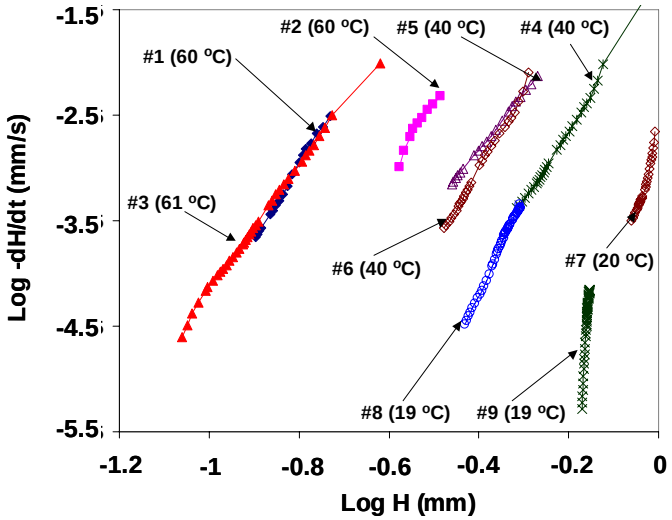

Figure 8. Differential method of analysis. Double log plots to derive power-law exponent n for power-law fluid

Pursuing the differential method, we calculated numerically the values of $-dH/dt$ using a moving 5-point quadratic applied to both $H(t)$ vs. t and log $H(t)$ vs. t data sets. The values of $-dH/dt$ derived from these two were substantially the same, which verified the differentiation method. The double log plots corresponding to Figure 7 are shown in the Figure 8.

Table 1. Summary of power-law constants derived from squeeze-flow and from dynamic data.

		Differential method		Integral method		Dynamic data	
Site #	Temperature, °C	*m*	*n*	*m*	*n*	*m*	*n*
1	60	890	0.566	878	0.526	1130	0.645
2	60	2100	1.289	1271	0.545		
3	61	1280	0.750	1270	0.745		
4	40	7180	0.579	7070	0.572	10900	0.590
5	40	8010	0.751	8723	0.803		
6	40	10100	0.654	10007	0.647		
7	20	15700	0.211	16650	0.223	39500[a]	0.565[a]
8	19	42000	0.375	35900	0.345		
9	19	8600	0.028	15383	0.122		

[a] Actual temperature = 30 °C

The integral method proved to be surprisingly robust. Convergence was obtained easily even with the initial gap as an unknown parameter. The results for the two methods are listed in Table 1. For both the dynamic and squeeze-flow data, the power-law exponent *m* tended to increase with temperature, i.e., the material became more Newtonian. This is an expected result. Within the experimental error, the dynamic and squeeze-flow results at 40 and 60 °C were indistinguishable. Running the asphalt on the rheometer at 20 C proved to be difficult, but the dynamic results at 30 °C suggest that the squeeze-flow test tends to give viscosities that are too low, and with excessive pseudoplasticity. Slip is a possible cause, and certainly the mold release used to prepare the samples may promote slippage.

Figure 9 displays a comparison between the results obtained using a combinatorial setup and those obtained using a parallel plate rheometer under dynamic mode. The curves containing symbols connected by lines are the viscosity curves obtained from squeeze flow setup, while the curves represented by symbols without any line are values for the magnitude of complex viscosities obtained using parallel plate. The samples at 40 ^{o}C and 60 ^{o}C covered a shear rate range of one decade whereas samples at 20 ^{o}C covered a shear rate range of more than two decades. At elevated temperatures the samples did not retain

their initial diameter and also squeezed out of the discs due to low viscosity. This reduced the number of available data point for the calculations, which in turn reduced the available shear-rate range. The limitations can be overcome by improving the setup where one can incorporate a larger disc such that the samples do not squeeze out.

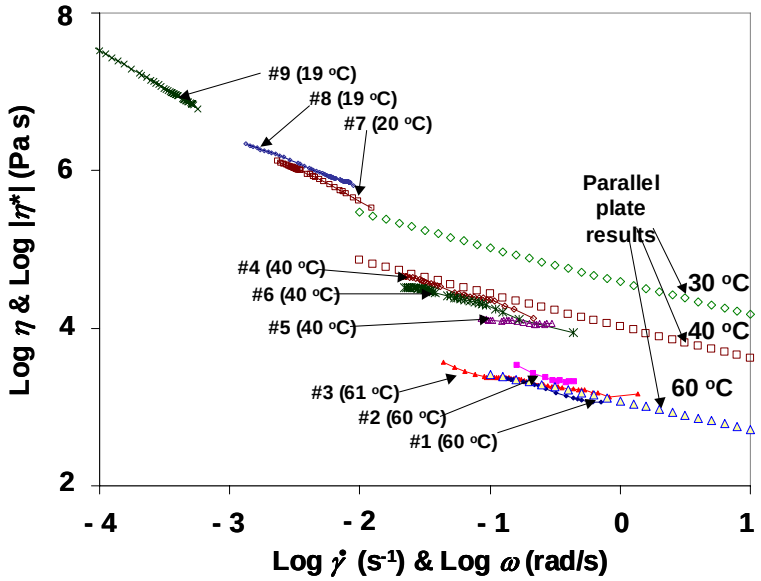

Figure 9. Comparison of viscosity results obtained from combinatorial rheometer with the magnitude of the complex viscosity obtained using parallel-plate fixtures in an ARES rheometer.

The results obtained from the parallel plate rheometer show that asphalt exhibits nearly perfect power-law behavior. Hence a power-law approximation for the squeeze flow analysis is a reasonable one. The irregular nature of the viscosity curves obtained for different samples using the combinatorial apparatus is due to the fact that these curves are constructed point-by-point from raw sample thickness data and values of the differential at each thickness. The integral method yields only the power-law parameters, and thus a continuous straight line on the log-log plot. For clarity, these are not shown.

The viscosity curves obtained at 60 ^{o}C from the combinatorial setup agree well with the dynamic data at the same temperature. That the viscosity data for the three samples do not overlap which could be due to the error involved in the force calculations. The viscosity curves at 40 ^{o}C from the combinatorial setup are close to the dynamic data. For this array the sample at the center experienced the highest force amongst the nine samples. The viscosity curve for this sample is lower than the parallel plate, which again could be due to error in force computation. The viscosity curve for the center sample has different slope compare to the other two samples at similar temperature. This could be due to non-uniform squeeze flow, because the top glass plate is floating on the sample and could tilt during squeeze flow. A tilt may also develop during the annealing step, or the sample may simply be off center. For samples that do not reach the edge, the degree of tilt can be determined after the run, and corrections for slightly tilted plates have been published.[29]

For the highly viscous samples, more motion of the plates can be achieved by thorough lubrication, perhaps with a fluorocarbon oil. The deformation then becomes uniform biaxial, and can be analyzed with viscoelastic constitutive models, an advantage.

As mentioned in the Introduction, the combinatorial method has a huge advantage over single-sample rheometers in that it can test a large array of test units simultaneously. The present design poses no particular limitations on the size of the array. By using a vacuum applied under a membrane, the forces on all elements are balanced and thus do not add as the array becomes larger. There are some aspects that do become more complicated with larger arrays. For example, because the volume to be evacuated grows with the array size, more vacuum ports and multiple vacuum lines would be needed to apply force to the samples simultaneously and rapidly. Power requirements for the heaters and coolers would grow also roughly with area. But most importantly, the gathering of sample area data using optical means becomes cumbersome. It would be necessary to have the array moved under the camera with an x-y positioning device as opposed to imaging the entire array at once. Clearly also it would be necessary to incorporate automatic image analysis to record the huge amount of data.

Some modifications of the design were considered. For example, direct measurement of the gap could be achieved by capacitive coupling of electrodes in the bottom plate by the top plate. The capacitance of the cell would increase strongly as the gap decreased. Magnetic coupling of embedded coils is another possibility, and would have the advantage that the calibration would be fairly independent of the composition of the sample.

Envisioned application to asphalt grading would involve the placement on the array of many freshly supplied samples, plus standard asphalts (such as the ones used for this study). From the results, the new samples that were promising would be shifted to the more conventional certification, while those that failed the screening would be reformulated or returned to the supplier.

Conclusions:

Based on the squeeze flow technique, we have successfully demonstrated a method for parallel rheological characterization of materials. The results obtained using combinatorial rheometer for asphalt samples at different temperature are consistent with the conventional single-sample rheometer. The existing combinatorial setup could only cover a shear rate range of about one decade at elevated temperatures. However the setup being very simple, one can easily fabricate another one, which can accommodate bigger samples to cover a wide shear rate range. The vacuum applied could had been increased or decreased to achieve different shear rates, but still it could not had covered more than a decade of shear rate. While squeezing flow can achieve a wide shear rate by selecting suitable sample size and the applied force, the present combinatorial design limits the range of both these variables because of the method of applying force and measuring the sample thickness. Problems with non-parallelism were experienced, but symmetry suggests that these may be minimized as the array is expanded. While the asphalt

samples provided optimal optical contrast, it was also shown that transparent materials can be characterized.

References:

(1) Dickie, J. P.; Yen, T. F. *Analytical Chemistry* **1967**, *39*, 1847-1852.

(2) Maruska, H. P.; Rao, B. M. L. *Fuel Science and Technology* **1987**, *5*, 119-168.

(3) Officials, A. A. o. S. H. a. T., in *Standard specification for performance graded asphalt binder*; 1-4 ed., 2002.

(4) Corbett, L. W.; Schweyer, H. E. *Asphalt Paving Technology* **1981**, *50*, 571-582.

(5) Lin, M.-S.; Chaffin, J. M.; Liu, M.; Glover, C. J.; Davison, R. R.; Bullin, J. A. *Fuel Science & Technology International* **1996**, *14*, 139-162.

(6) Summarized in R.E. Robertson, e. a. **2001**, *1*.

(7) Pathak, J. A.; Berg, R. F.; Beers, K. L. *Abstracts of Papers, 230th ACS National Meeting, Washington, DC, United States, Aug. 28-Sept. 1, 2005* **2005**, PMSE-559.

(8) Peek, R. L., Jr. *J. Rheology* **1932**, *3*, 345-372.

(9) Scott, J. R. *J. Rubber Research* **1945**, *14*, 195-198.

(10) Dienes, G. J. *Journal of Colloid Science* **1949**, *4*, 257-264.

(11) Scott, J. R. *Rubber Chemistry and Technology* **1946**, *19*, 461-465.

(12) Gent, A. N. *British Journal of Applied Physics* **1960**, *11*, 85-87.

(13) Leider, P. J.; Bird, R. B. *Industrial & Engineering Chemistry Fundamentals* **1974**, *13*, 336-341.

(14) Leider, P. J. *Industrial & Engineering Chemistry Fundamentals* **1974**, *13*, 342-346.

(15) Marshall, D. I. *ASTM Bulletin* **1955**, *No. 204*, 40-44.

(16) Arai, T.; Nakakuki, A.; Akimoto, S.; Aoyama, H. *Kogyo Kagaku Zasshi* **1960**, *63*, 427-434.

(17) Goto, K.; Kawai, R. *Kogakuin Daigaku Kenkyu Hokoku* **1976**, *41*, 26-31.

(18) Burns, R.; Gandhi, K. S. *Proceedings of the Annual Conference - Reinforced Plastics/Composites Institute, Society of the Plastics Industry* **1977**, *32*, Sect. 7C, 8 pp.

(19) Shaw, M. T. *Polymer Engineering and Science* **1977**, *17*, 266-268.

(20) Kataoka, T.; Kitano, T.; Nishimura, T. *Rheologica Acta* **1978**, *17*, 626-631.

(21) Bloechle, D. P. *Technical Papers - Society of Plastics Engineers* **1978**, *24*, 641-644.

(22) Whiting, R.; Jacobsen, P. H. *Journal of Materials Science* **1979**, *14*, 307-311.

(23) Lohr, J. *Plasty a Kaucuk* **1983**, *20*, 234-235.

(24) Winther, G.; Kramer, O. *Polymer Testing* **1991**, *10*, 161-174.

(25) Winther, G.; Larsson, I.; Kramer, O. *Polymer Testing* **1991**, *10*, 263-272.

(26) Lohr, J.; Mejzr, I.; Pokorny, P. In *Czech.*; (Synpo S.P., Czech.). Cs, 1992, p 4 pp.

(27) http://www.caplab.uconn.edu/ti/CAPLab/index.html

(28) Laun, H. M. *Makromolekulare Chemie, Macromolecular Symposia* **1992**, *56*, 55-66.

(29) Hoffner, B. C., Q.H. Corradini, M.G. Peleg M. *Rheologica Acta* **2001**, *40*, 289-295.